$M_2(SeO_3)F_2$ (M = Zn, Cd): Understanding the structure directing effect of $[SeO_3]^{2-}$ groups on constructing ordered oxyfluorides

Fengguang You,[a,b,#] Pifu Gong, [a,#] Fei Liang,[a,b,#] Xingxing Jiang,[a] Heng Tu,[a] Ying Zhao,[a] Zhanggui Hu[*,c] and Zheshuai Lin[*,a,b]

[a] Key Lab of Functional Crystals and Laser Technology, Technical Institute of Physics and Chemistry, Chinese Academy of Sciences, Beijing 100190, China

[b] University of Chinese Academy of Sciences, Beijing 100190, China

[c] Institute of Functional Crystal Materials, Tianjin University of Technology, Tianjin 300384, China

Table of Contents

Experimental Procedures

Synthesis

All of the starting chemicals were analytical grade from commercial source. K_2CO_3 (Guangdong Xilong Chemical Co., Ltd., 99%), SeO_2 (Aladdin Industrial Corporation, 99%), $Zn(NO_3)_2 \cdot 6H_2O$ (Tianjin Fuchen Chemical reagent co. Ltd, 99%), $Cd(NO_3)_2 \cdot 4H_2O$ (Alfa Aesar, 98.5%) and HF (Guangdong Xilong Chemical Co., Ltd., 40%) were used as received. Single crystals of $M_2(SeO_3)F_2$ (M=Zn, Cd) were prepared by hydrothermal reactions. For $Zn_2(SeO_3)F_2$, 0.3455 g (2.5 mmol) of K_2CO_3, 0.2975 g (1 mmol) of $Zn(NO_3)_2 \cdot 6H_2O$, 0.333 g (3 mmol) of SeO_2, and 2.0 mL of HF were combined. For $Cd_2(SeO_3)F_2$, 0.3455 g(2.5mmol) of K_2CO_3, 0.3085 g(1mmol) of $Cd(NO_3)_2 \cdot 4H_2O$, 0.333 g(3mmol) of SeO_2, and 2.0 mL of HF were combined. The respective solutions were placed in 23 mL Teflon-lined autoclaves that were subsequently sealed. The autoclaves were gradually heated to 230°C, held at this temperature for 4 days, and cooled slowly to room temperature at a rate of 3 °C/h. After that, autoclaves were opened and the products were recovered by filtration, which were further washed with distilled water to remove soluble solids and dried in an oven at 60°C. Colorless blocks crystals for $Zn_2(SeO_3)F_2$, and $Cd_2(SeO_3)F_2$ were obtained in yield of about 70% and 62%, (based on Zn or Cd) respectively.

Characterization

Single-crystal XRD measurement. Small crystals with sizes about $0.1 \times 0.1 \times 0.08$ mm^3 for $M_2(SeO_3)F_2$ (M = Zn, Cd) were picked for structure resolution using the single-crystal X-ray diffraction method. The diffraction data were collected on a Rigaku AFC10 single-crystal diffractometer equipped with graphite-monochromated Mo Kα radiation (λ = 0.71073 Å) at 153 K. The crystal structures were solved by direct methods with the program SHELXTL and refined by full-matrix least squares on F^2 by SHELXTL programs[1, 2]. The structures were verified using the ADDSYM algorithm from the program PLATON, and no higher symmetry was found. The relevant crystallographic data, selected bond lengths and angles are listed in Table S1 and Table S2.

Powder XRD analysis. Powder X-ray diffraction (PXRD) of the polycrystalline materials were performed at room temperature using an automated Bruker D8 Focus X-ray diffractometer equipped with a diffracted monochromator set for Cu Kα (λ=1.5418 Å) radiation. The scanning step width of 0.02° and the scanning rate of 0.4°s^{-1} were applied to record the patterns in the 2 theta range of 10-70°.

Low-temperature powder X-ray diffraction. Variable temperature X-ray diffraction patterns were recorded from the 6K to 284K with the internal of 20K. Each pattern was written down with D/Max-2400(Rint), Rigaku X-ray diffractometer Cu Kα radiation on the finely grounded powder samples. The angular scanning range were set to 10° to 70° with a step of 0.02° and scanning rate 0.5s/step. The cell parameters under different temperature were refined by Rietveld method using TOPAS 4.2 program[3].

UV-Vis Diffuse Reflectance Spectroscopy. The diffuse reflectance data for the title compounds were collected with a Varian Cary 7000 UV–vis–NIR spectrometer equipped with an integrating sphere in the wavelength range from 200 to 2500 nm. $BaSO_4$ was employed as the 100% reflectance standard.[4]

Infrared (IR) Spectroscopy. IR spectra were recorded on a Magna 750 FT-IR spectrometer as KBr pellets in the range of 4000-450 cm^{-1}.

Raman Spectroscopy. The grinded pure phase powder samples were first placed on an objective slide, and a Renishaw invia raman microscope with 532 nm excitation wavelength was used to record the Raman spectra.

Thermal Analysis. Thermogravimetric analysis (TGA) was performed on a SDT-Q600 TG-DTA Thermogravimetric Analyzer. The sample was placed in a alumina crucible, which was heated at a rate of 15 °C/min under N_2 flow from room temperature to 1000 °C.

Computational method

The first-principles calculations for the $M_2(SeO_3)F_2$ (M = Zn, Cd) crystals are performed by the plane-wave pseudopotential method implemented in the CASTEP package based on the density functional theory (DFT).[5] The ion-electron interactions are modeled by the optimized normal-conserving pseudopotentials for all elements.[6] The Perdew, Burke and Ernzerhof (PBE) functionals of generalized gradient approximation (GGA) are adopted to describe the exchange-correlation (XC) functionals.[7, 8] The kinetic energy cutoffs of 900 eV and Monkhorst-Pack k-point meshes[9] with density of 3×2×5 and 3×2×4 points in the Brillouin zone are chosen for $Zn_2(SeO_3)F_2$ and $Cd_2(SeO_3)F_2$, respectively. On the basis of the scissor-corrected electron band structure, the refractive index n and birefringence Δn can be obtained by the real part of dielectric function based on the Kramers-Kronig transform[10, 11]. The phonon spectra calculations are carried out based on the linear response method and the convergence tolerance of $1×10^{-9}$ ev/$Å^2$ are chosen[12]. Our tests reveal that the above computational set ups are sufficiently accurate for present purposes.

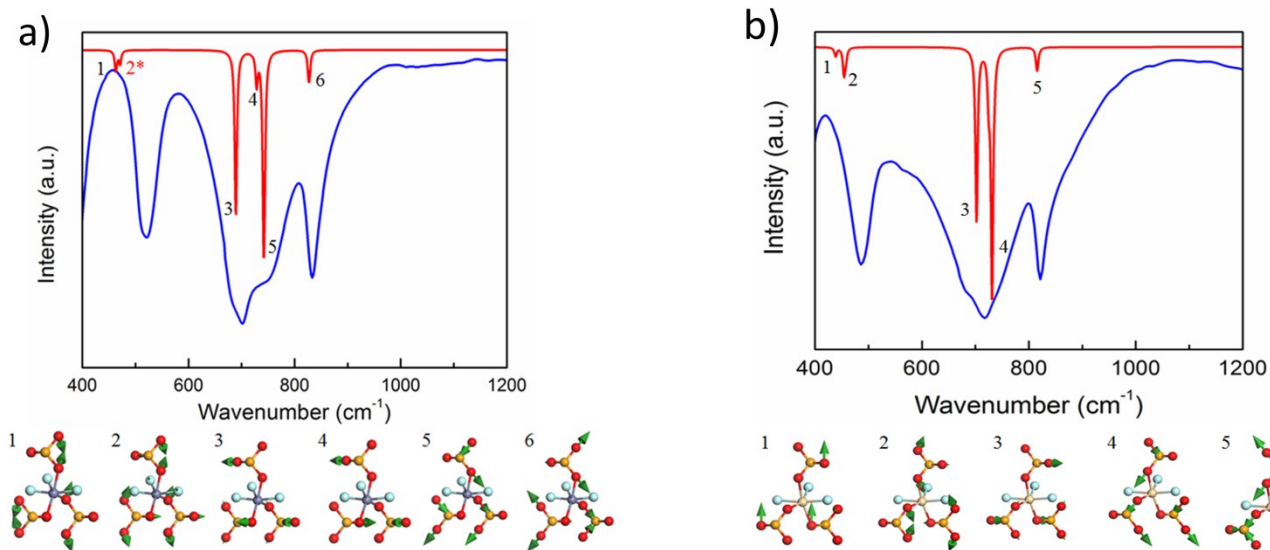## Results and Discussion
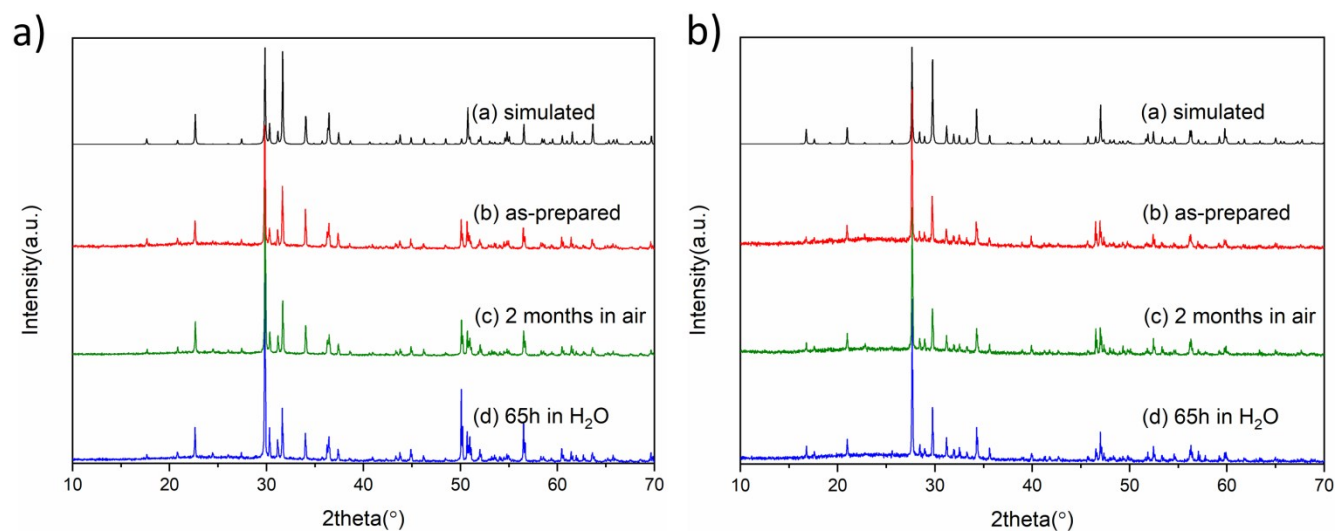
Figure S1. PXRD patterns of $Zn_2(SeO_3)F_2$ (a) and $Cd_2(SeO_3)F_2$ (b). The top and bottom panels show the simulated and measured XRD.
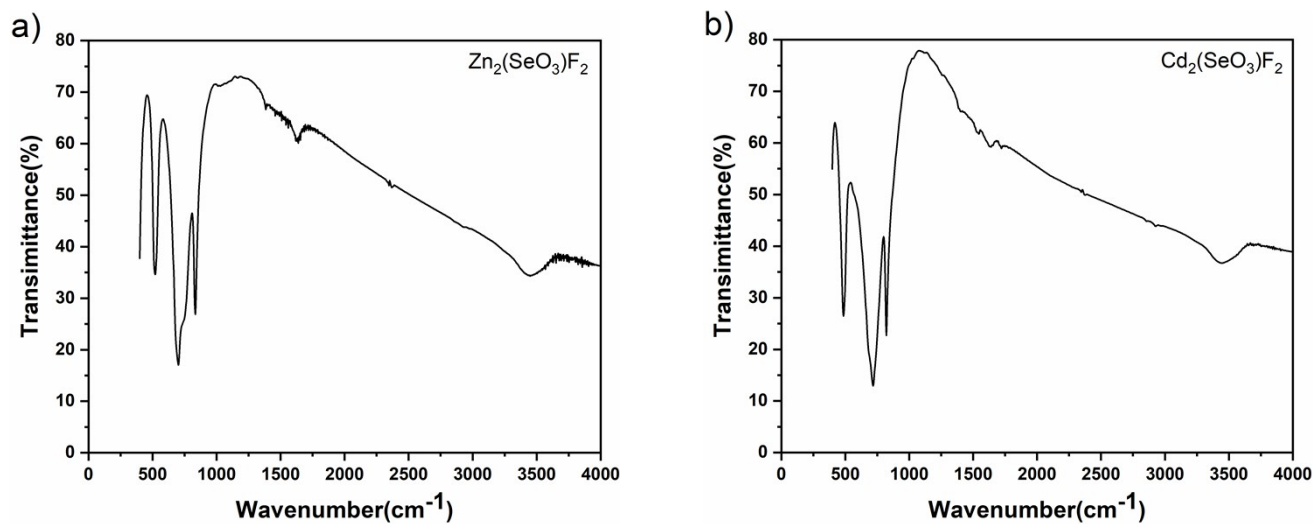
Figure S2. IR spectra of (a) $Zn_2SeO_3F_2$ and (b) $Cd_2SeO_3F_2$.

Figure S3. The experimental and simulated IR spectra of (a) $Zn_2SeO_3F_2$ and (b) $Cd_2SeO_3F_2$ (top graph); Assignments of peaks and the corresponding vibrational mode in the range of 400-1200 cm-1 in the Infrared absorption spectra (bottom graph).
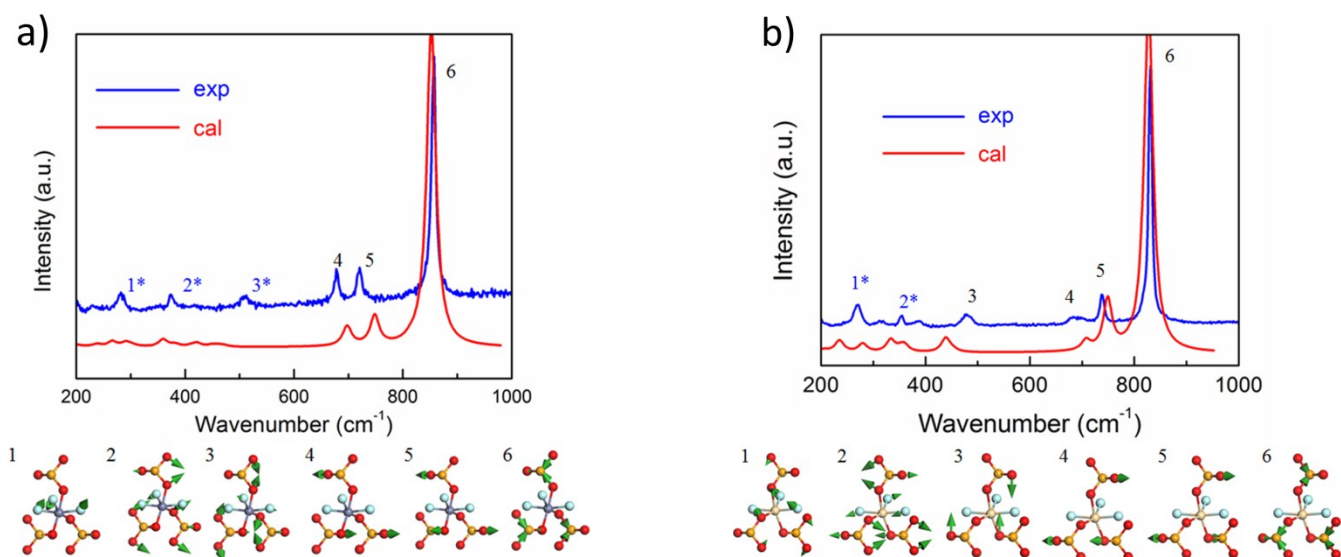
Figure S4. The experimental and simulated Raman spectra of (a) $Zn_2SeO_3F_2$ and (b) $Cd_2SeO_3F_2$ (top graph); Assignments of peaks and the corresponding vibrational mode in the range of 200-1000 cm-1 in the Raman spectra (bottom graph).
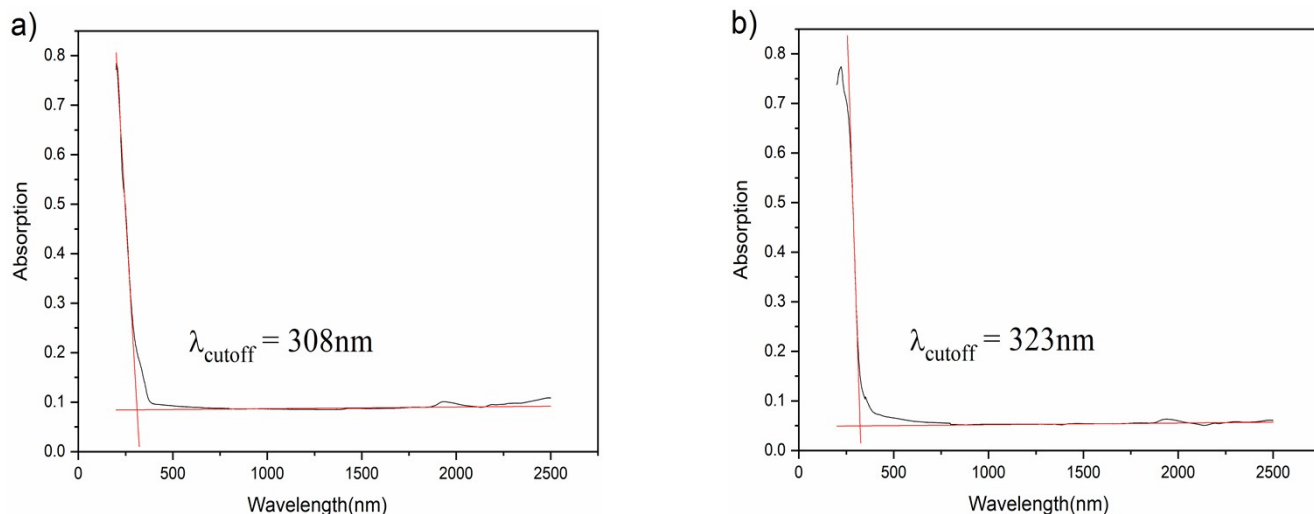
Figure S5. The UV–Vis–NIR diffuse-absorb spectra of (a) $Zn_2SeO_3F_2$ and (b) $Cd_2SeO_3F_2$.

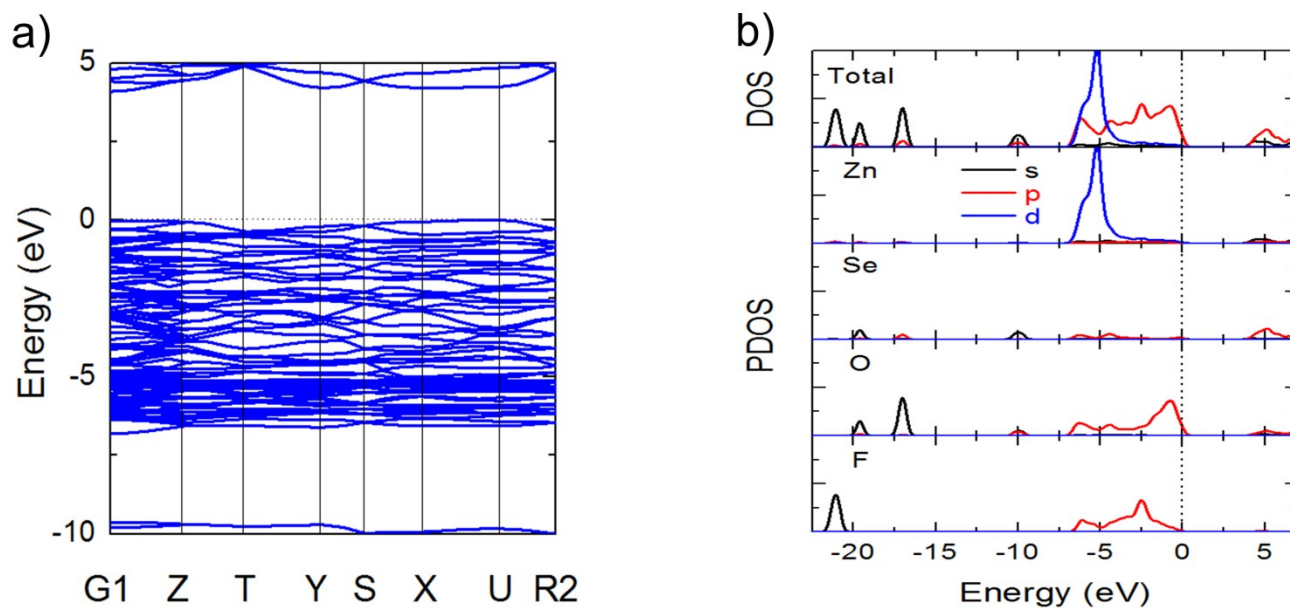
Figure S6. The calculated (a) electronic band structure with an indirect gap and (b) the PDOS projected on the constituent elements of $Zn_2(SeO_3)F_2$. The region lower than -5 eV is consisted of the isolated inner-shell states with Zn $4s$, Se $4s$, O $2s$ and F $2s$ orbitals, which have little interaction with neighbour atoms. The upper part of valence bands (VB) are mainly composed of the p orbitals of selenium ($4p$), zinc ($4p$), fluorine ($2p$), and oxygen ($2p$), indicating the strong interaction between these atoms. The states at the bottom of conduction bands (CB) are mainly contributed from the orbitals of Zn, Se and O.
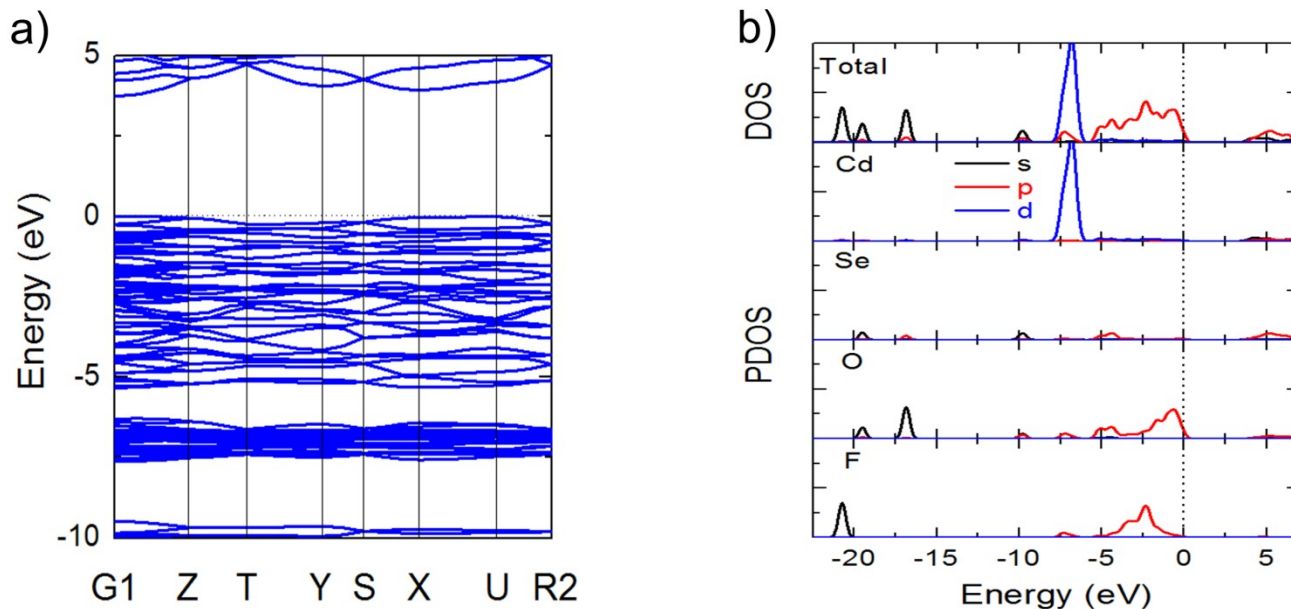
Figure S7. The calculated (a) electronic band structure with an direct gap and (b) the PDOS projected on the constituent elements of $Cd_2(SeO_3)F_2$. The region lower than -5 eV is consisted of the isolated inner-shell states with Cd $5s$, Se $4s$, O $2s$ and F $2s$ orbitals, which have little interaction with neighbour atoms. The upper part of valence bands (VB) are mainly composed of the p orbitals of selenium ($4p$), cadmium ($5p$), fluorine ($2p$), and oxygen ($2p$), indicating the strong interaction between these atoms. The states at the bottom of conduction bands (CB) are mainly contributed from the orbitals of Cd, Se and O.
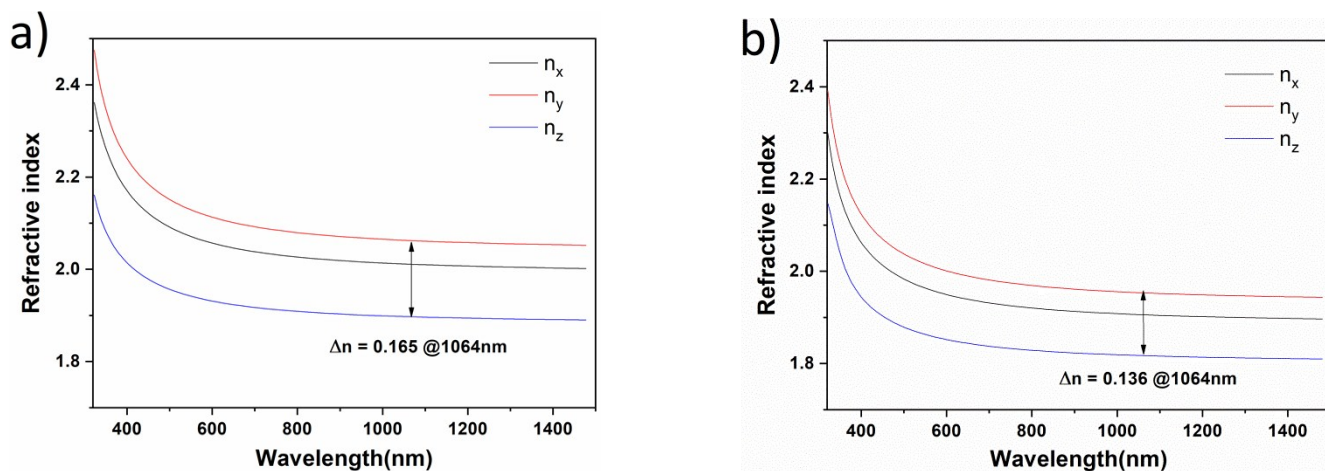
Figure S8. The refractive indices of (a) $Zn_2SeO_3F_2$ and (b) $Cd_2SeO_3F_2$.

Table S1. Crystallographic data and Refinement results for $M_2(SeO_3)F_2$ (M = Zn, Cd)

Formula	$Zn_2(SeO_3)F_2$	$Cd_2(SeO_3)F_2$
Formula weight	295.7	389.76
Temperature/K	153(2)	153(2)
Crystal system	orthorhombic	orthorhombic
Space group	Pnma	Pnma
a/Å	7.2758(15)	7.8033(16)
b/Å	10.042(2)	10.566(2)
c/Å	5.2562(11)	5.7294(11)
α/°	90	90
β/°	90	90
γ/°	90	90
Volume/Å^3	384.03(14)	472.39(16)
Z	4	4
ρ_{cal}g/cm^3	5.114	5.48
μ/mm^{-1}	21.905	16.656
F(000)	544	688
Crystal size/mm^3	0.1 × 0.1 × 0.08	0.1 × 0.1 × 0.08
Radiation	MoKα (λ = 0.71073)	MoKα (λ = 0.71073)
2θ range for data collection/°	8.12 to 51.96	8.1 to 54.94
Index ranges	-8 ≤ h ≤ 8, -10 ≤ k ≤ 12, -6 ≤ l ≤ 6	-10 ≤ h ≤ 7, -13 ≤ k ≤ 13, -5 ≤ l ≤ 7
Reflections collected	2426	2630
Independent reflections	393 [R_{int} = 0.0410, R_{sigma} = 0.0228]	567 [R_{int} = 0.0548, R_{sigma} = 0.0358]
Data/restraints/parameters	393/0/40	567/0/40
Goodness-of-fit on F^2	1.254	1.246
Final R indexes [I⩾2σ (I)]^a	R_1 = 0.0242, wR_2 = 0.0621	R_1 = 0.0343, wR_2 = 0.0824
Final R indexes [all data]	R_1 = 0.0244, wR_2 = 0.0622	R_1 = 0.0354, wR_2 = 0.0830
Largest diff. peak/hole / e Å^{-3}	0.69/-1.10	1.41/-2.47

^{a} R(F) $=\sum||F_o|-|F_c||/\sum|F_o||$ for $F_o{}^2 > 2\sigma(F_o{}^2)$ and $Rw(F_o{}^2) =\{\sum[w(F_o{}^2-F_c{}^2)^2]/\sum wF_o{}^4\}^{\frac{1}{2}}$ for all data. $w^{-1} = \sigma^2(F_o{}^2) +(zP)^2$, where $P=(Max(F_o{}^2, 0) +2 F_c{}^2)/3$

Table S2. Selected bond lengths (Å) and bond angles (deg) for $M_2(SeO_3)F_2$ (M = Zn, Cd).

Zn2(SeO3)F2

Zn(1)-F(3)#2	2.073(3)	F(3)-Zn(1)-O(4)	92.28(17)	F(3)#2-Zn(1)-F(3)#3	77.14(12)
Zn(1)-F(3)	2.051(3)	F(3)#2-Zn(1)-O(5)#4	86.81(12)	F(3)-Zn(1)-F(3)#3	96.12(7)
Zn(1)-F(3)#3	2.090(3)	F(3)-Zn(1)-O(5)#4	82.18(12)	F(3)-Zn(1)-F(3)#2	167.63(17)
Zn(1)-O(4)	2.061(3)	F(3)#3-Zn(1)-O(5)#4	84.54(12)	O(4)-Zn(1)-O(5)#4	174.42(17)
Zn(1)-O(5)#4	2.138(4)	O(4)-Zn(1)-F(3)#3	96.76(15)	O(5)#5-Zn(1)-O(4)	101.82(16)
Zn(1)-O(5)#5	2.033(3)	O(4)-Zn(1)-F(3)#2	98.77(17)	O(5)#5-Zn(1)-O(5)#4	77.99(15)
Se(2)-O(4)	1.740(5)	O(5)#5-Zn(1)-F(3)#3	158.66(13)		
Se(2)-O(5)#1	1.696(3)	O(5)#5-Zn(1)-F(3)#2	89.64(13)		
Se(2)-O(5)	1.696(3)	O(5)#5-Zn(1)-F(3)	93.56(13)		

Cd2(SeO3)F2

Cd(1)-F(3)	2.220(4)	F(3)-Cd(1)-O(4)#1	93.33(15)	F(3)-Cd(1)-F(3)#2	98.95(8)
Cd(1)-F(3)#1	2.249(4)	F(3)#2-Cd(1)-O(4)#1	155.60(15)	F(3)-Cd(1)-F(3)#1	170.2(2)
Cd(1)-F(3)#2	2.244(4)	F(3)-Cd(1)-O(4)#3	81.26(15)	F(3)#2-Cd(1)-F(3)#1	76.08(14)
Cd(1)-O(4)#1	2.263(4)	F(3)#1-Cd(1)-O(4)#1	88.44(15)	O(5)-Cd(1)-O(4)#1	106.12(18)
Cd(1)-O(4)#3	2.327(4)	F(3)#2-Cd(1)-O(4)#3	82.88(15)	O(5)-Cd(1)-O(4)#3	172.27(18)
Cd(1)-O(5)	2.237(3)	F(3)#1-Cd(1)-O(4)#3	89.71(15)	O(4)#1-Cd(1)-O(4)#3	78.23(16)
Se(2)-O(4)	1.689(4)	F(3)-Cd(1)-O(5)	92.0(2)		
Se(2)-O(4)#4	1.689(4)	O(5)-Cd(1)-F(3)#2	94.50(19)		
Se(2)-O(5)	1.723(6)	O(5)-Cd(1)-F(3)#1	96.7(2)		

Table S3. Bond valence analysis of $M_2(SeO_3)F_2$ (M = Zn, Cd)

Atom	Coord	D_aver Sigm	Distort(x10-4)	Valence	BVSum(Sigma)
Se2	3	1.7104(23)	1.475	4	3.943(24)
Zn1	6	2.0745(12)	2.627	2	1.987(7)
F3	3	2.0714(18)	0.618	-1	0.887(4)
O4	3	1.9540(21)	60.086	-2	1.974(18)
O5	3	1.9557(19)	93.172	-2	2.085(13)

Atom	Coord	D_aver Sigm	Distort(x10-4)	Valence	BVSum(Sigma)
Cd1	6	2.2566(16)	2.254	2	2.052(9)
Se2	3	1.7005(31)	0.892	4	4.048(33)
F3	3	2.2377(21)	0.336	-1	0.947(5)
O4	3	2.0928(25)	187.541	-2	2.089(17)
O5	3	2.0659(29)	137.583	-2	2.080(25)

Table S4. Cell parameters of $Zn_2(SeO_3)F_2$ at various temperatures.

Temperature (K)	Cell parameter (Å)		
	a	b	c
6	7.27169	10.03445	5.25457
25	7.27161	10.03442	5.25457
44	7.27173	10.03486	5.25481
65	7.2719	10.03535	5.25523
84	7.27235	10.03619	5.25596
105	7.27301	10.03733	5.25688
125	7.27369	10.03838	5.25786
145	7.27441	10.03966	5.25893
165	7.27553	10.0413	5.2603
185	7.27642	10.04274	5.26149
204	7.27752	10.04424	5.26286
225	7.27894	10.04626	5.26442
245	7.28038	10.04818	5.266
264	7.28179	10.05026	5.26762
284	7.28315	10.05221	5.26919

References

(1)   Sheldrick, G. M. A short history of SHELX. *Acta Crystallographica Section A* **2008,** 64, 112-122

(2)   Sheldrick, G. SHELXTL, version 6.14; Bruker Analytical X-ray Instruments. *Inc.: Madison, WI* **2003**,

(3)   Bruker AXS TOPAS V4: General profile and structure analysis software for powder diffraction data. User's manual, Bruker AXS, Karlsruhe, Germany **2008**. *Bruker AXS TOPAS V4: General profile and structure analysis software for powder diffraction data. User's manual*, Bruker AXS, Karlsruhe, Germany **2008**.

(4)   Kubelka, P.; Munk, F. An article on optics of paint layers. *Z. Tech. Phys* **1931,** 12 (593-601),

(5)   Clark, S. J.; Segall, M. D.; Pickard, C. J.; Hasnip, P. J.; Probert, M. J.; Refson, K.; Payne, M. C. First principles methods using CASTEP. *Zeitschrift Fur Kristallographie* **2005,** 220 (5-6), 567-570

(6)   Hamann, D. R.; Schluter, M.; Chiang, C. Norm-Conserving Pseudopotentials. *Phys. Rev. Lett.* **1979,** 43 (20), 1494-1497

(7)   Hammer, B.; Hansen, L. B.; Norskov, J. K. Improved adsorption energetics within density-functional theory using revised Perdew-Burke-Ernzerhof functionals. *Physical Review B* **1999,** 59 (11), 7413-7421

(8)   Perdew, J. P.; Burke, K.; Ernzerhof, M. Generalized gradient approximation made simple. *Phys. Rev. Lett.* **1996,** 77 (18), 3865-3868

(9)   Monkhorst, H. J.; Pack, J. D. Special Points For Brillouin-Zone in Integrations. *Physical Review B* **1976,** 13 (12), 5188-5192

(10)   Lin, J.; Lee, M. H.; Liu, Z. P.; Chen, C. T.; Pickard, C. J. Mechanism for linear and nonlinear optical effects in beta-BaB2O4 crystals. *Phys Rev B* **1999,** 60 (19), 13380-13389

(11)   Jing, Q.; Dong, X. Y.; Chen, X. L.; Yang, Z. H.; Pan, S. L.; Lei, C. The lone-pairs enhanced birefringence and SHG response: A DFT investigation on M2B5O9Cl (M = Sr, Ba, and Pb). *Chem Phys* **2015,** 453, 42-46

(12)   Yao, Y.; Tse, J. S.; Sun, J.; Klug, D. D.; Martonak, R.; Iitaka, T. Comment on "New metallic carbon crystal". *Phys Rev Lett* **2009,** 102 (22), 229601